NON-ORDINARY STATE-BASED PERIDYNAMIC

www.pmass.io

Introduction

This document provides the background knowledge on the non-ordinary state-based peridynamic (NOSB-PD) theory in the discretized form. Refer to [1-10] for further formulations and their derivatives. Due to the convenient introduction of traditional constitutive models, the NOSB-PD has great advantages in material nonlinear analysis and fracture simulation, and has attracted broad attention in the computational fracture mechanics community

Non-Ordinary State-Based Peridynamics (NOSB-PD) vs Bond-Based Peridynamics (BB-PD)

The balance of linear momentum in peridynamics takes an integral form, whereas partial derivatives are used in the classical continuum mechanics. Therefore, the equation of motion in peridynamics valid everywhere in the material despite of presence of discontinuities such as cracks. The peridynamics (PD) discretize the material body into a defined number of points, and the kinetics of materials is represented by the bonds between the points. During the early development of peridynamics, the bond-based peridynamics (BB-PD) is developed where the kinetic energy of a given point xi is obtained by a summation of forces from bonds between the point $\mathbf{x_i}$ and each point in a finite distance (referred to as "Horizon) as shown in Fig. 1a. In the development of NOSB-PD, however, the kinetics of point $\mathbf{x_i}$ is not only a function of bond relationships with points within its horizon (H_i) but also depends on bonds in the horizon of point $\mathbf{x_j}$ (H_j) as shown in Fig. 1b. The adjustment enables NOSB-PD to capture material response with any Poisson's ratio [1] by allowing interactions between bonds.

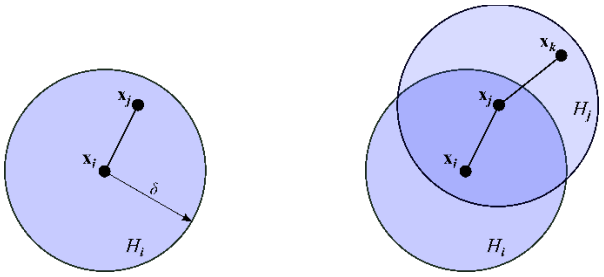

(a) (b)

Figure 1. Peridynamic bonds: (a) BB-PD vs. (b) NOSB-PD.

NOSB-PD Formulation

The kinematics of peridynamics for a two-dimensional body is illustrated in Fig. 2. A point located at position $\mathbf{x_i}$ interacts with its surrounding points within an area of influence, the so-called "horizon", where δ is the horizon size. In NOSB-PD, vector-states are introduced to describe the kinematics of the body (see Fig. 2). The position vector-state $\mathbf{X}$, also called the bond $\boldsymbol{\xi}$, from the perspective of $\mathbf{x_i}$, is defined as the relative position of $\mathbf{x_i}$ and $\mathbf{x_j}$ in the reference configuration B_0.

$$\mathbf{X}\langle \mathbf{x_j} - \mathbf{x_i} \rangle = \boldsymbol{\xi_{ij}} = \mathbf{x_j} - \mathbf{x_i} \tag{1}$$

The deformation vector-state, Y, represents the bond in the deformed body B.

$$\mathbf{Y}\langle \mathbf{x_j} - \mathbf{x_i} \rangle = \boldsymbol{\xi_{ij}} + \boldsymbol{\eta_{ij}} = \mathbf{y_j} - \mathbf{y_i} \tag{2}$$

where $\mathbf{y_i} = \mathbf{x_i} + \mathbf{u_i}$ and $\mathbf{y_j} = \mathbf{x_j} + \mathbf{u_j}$. $\mathbf{u_i}$ and $\mathbf{u_j}$ are deformations corresponding to $\mathbf{x_i}$ and $\mathbf{x_j}$, respectively. $\boldsymbol{\eta_{ij}} = \mathbf{u_j} - \mathbf{u_i}$ is the relative deformation. Note that the angle bracket, $\langle \quad \rangle$, is used to indicate that the state operates on the vector in $\langle \quad \rangle$. Also, indices indicate the correspondence of a variable to material points, $\mathbf{A_i}$

denotes the state $\mathbf{A}$ at point $\mathbf{x_i}$, or $\mathbf{A_{ij}}$ corresponds to the bond between $\mathbf{x_i}$ and $\mathbf{x_j}$. In NOSB-PD, the deformation vector-state, **Y**, takes the role of deformation gradient tensor, **F**, in classical local mechanics in describing kinematics of the body [21, 23]. Silling [23] introduced an approximation for evaluating the classical deformation gradient tensor in order to incorporate the classical constitutive equations in NOSB-PD.

$$\mathbf{F_i} = \left[\sum_{j=1}^{n_i} \omega_{ij}(\mathbf{y_j} - \mathbf{y_i}) \otimes (\mathbf{x_j} - \mathbf{x_i}) V_j\right] . \mathbf{K_i^{-1}} \tag{3}$$

where $\omega_{ij} = \omega(|\boldsymbol{\xi}_{ij}|)$ denotes an influence function, $\boldsymbol{n_i}$ is the number of points within the horizon of $\mathbf{x_i}$, and V_j is the volume of point $\mathbf{x_j}$. $\mathbf{K_i}$ is shape tensor, expressed as follows at point $\mathbf{x_i}$.

$$\mathbf{K_i} = \sum_{j=1}^{n_i} \omega_{ij}(\mathbf{x_j} - \mathbf{x_i}) \otimes (\mathbf{x_j} - \mathbf{x_i}) V_j \tag{4}$$

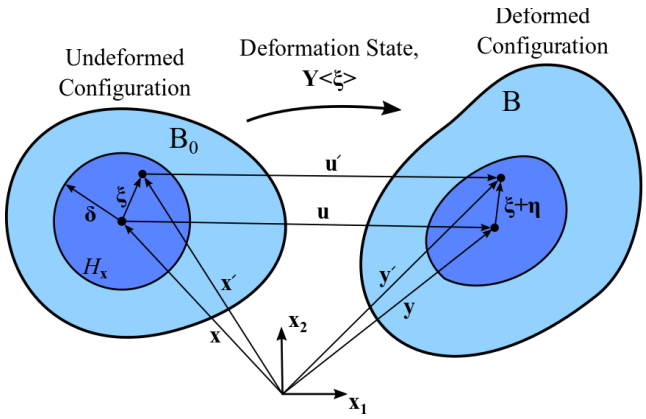

Figure 2. Peridynamic states: Position vector-state **X**, deformation vector-state **Y**, and force vector-state **T**.

In NOSB-PD, it is assumed that points interact through long-range forces represented by force vector-state **T** [23]. The steady-state equilibrium equations for point $\mathbf{x_i}$ is given by summation of force vector-states over the horizon of $\mathbf{x_i}$

$$\mathbf{K_i} = \sum_{j=1}^{n_i} \{\mathbf{T_i}\langle \mathbf{x_j} - \mathbf{x_i} \rangle - \mathbf{T_j}\langle \mathbf{x_i} - \mathbf{x_j} \rangle\} V_j + \mathbf{b_i} = \mathbf{0} \tag{5}$$

where **b** is the body force. The force vector-state is obtained from

$$\mathbf{T_i}\langle \mathbf{x_j} - \mathbf{x_i} \rangle = \omega_{ij} \boldsymbol{\sigma}_i \mathbf{K_i^{-1}} (\mathbf{x_j} - \mathbf{x_i}) \tag{6}$$

where $\boldsymbol{\sigma}$ is the first Piola-Kirchhoff stress and determined through material constitutive equation.

Force vector-state

The discretization of force vector-state is provided by Breitenfeld et al. [19], and Yaghoobi and Chorzepa [21]. This study presents a modified formulation for 2D plane stress and 3D problems. For linearly elastic materials with small deformations, the infinitesimal strain tensor $\boldsymbol{\varepsilon} = 0.5(\mathbf{F}^T + \mathbf{F}) - \mathbf{I}$ can be rewritten by definition of peridynamic deformation gradient tensor (Eq. 3) as

$$\boldsymbol{\varepsilon_i} = 0.5 \left[\sum_{j=1}^{n_i} \omega_{ij} \{(\mathbf{u_j} - \mathbf{u_i}) \otimes (\mathbf{x_j} - \mathbf{x_i}) + (\mathbf{x_j} - \mathbf{x_i}) \otimes (\mathbf{u_j} - \mathbf{u_i})\} V_j\right] . \mathbf{K_i^{-1}} \tag{7}$$

The infinitesimal strain tensor in vector (or Voigt) notation takes the following form,

$$\boldsymbol{\varepsilon_i} = \mathbf{K_i^*} \sum_{\boldsymbol{j=1}}^{\boldsymbol{n_i}} \omega_{ij} \mathbf{N}_{ij} \mathbf{U}_{ij} V_j \tag{8}$$

where for a 2D problem, $\mathbf{K}^*$ is a 3×4 matrix and stores the arrays of inverse of shape tensor $\mathbf{K}$.

$$\mathbf{K}^* = \begin{bmatrix} K_{11}^{-1} & 0 & K_{12}^{-1} & 0 \\ 0 & K_{12}^{-1} & 0 & K_{22}^{-1} \\ K_{12}^{-1} & K_{11}^{-1} & K_{22}^{-1} & K_{12}^{-1} \end{bmatrix} \quad \text{(2D)} \tag{9}$$

In 3D, $\mathbf{K}^*$ is a 6×9 matrix.

$$\mathbf{K}^* = \begin{bmatrix} K_{11}^{-1} & 0 & 0 & K_{21}^{-1} & 0 & 0 & K_{31}^{-1} & 0 & 0 \\ 0 & K_{12}^{-1} & 0 & 0 & K_{22}^{-1} & 0 & 0 & K_{32}^{-1} & 0 \\ 0 & 0 & K_{13}^{-1} & 0 & 0 & K_{23}^{-1} & 0 & 0 & K_{33}^{-1} \\ 0 & K_{13}^{-1} & K_{12}^{-1} & 0 & K_{23}^{-1} & K_{22}^{-1} & 0 & K_{33}^{-1} & K_{32}^{-1} \\ K_{13}^{-1} & 0 & K_{11}^{-1} & K_{23}^{-1} & 0 & K_{21}^{-1} & K_{33}^{-1} & 0 & K_{31}^{-1} \\ K_{12}^{-1} & K_{11}^{-1} & 0 & K_{22}^{-1} & K_{21}^{-1} & 0 & K_{32}^{-1} & K_{31}^{-1} & 0 \end{bmatrix} \quad \text{(3D)} \tag{10}$$

N is a 4 × 2 matrix for 2D problem and 9 × 3 for a 3D problem which formed from elements of position vector-state $\boldsymbol{\xi_{ij}} = \mathbf{x_j} - \mathbf{x_i} = [\xi_1, \xi_2]$ for 2D and $[\xi_1, \xi_2, \xi_3]$ for 3D, as show below:

$$\mathbf{N} = \begin{bmatrix} \xi_1 & 0 \\ 0 & \xi_1 \\ \xi_2 & 0 \\ 0 & \xi_2 \end{bmatrix} \quad \text{(2D)} \quad \text{and} \quad \mathbf{N} = \begin{bmatrix} \xi_1 & 0 & 0 \\ 0 & \xi_1 & 0 \\ 0 & 0 & \xi_1 \\ \xi_2 & 0 & 0 \\ 0 & \xi_2 & 0 \\ 0 & 0 & \xi_2 \\ \xi_3 & 0 & 0 \\ 0 & \xi_3 & 0 \\ 0 & 0 & \xi_3 \end{bmatrix} \quad \text{(3D)} \tag{11}$$

and $\mathbf{U_{ij}} = \mathbf{u_j} - \mathbf{u_i}$ is the relative deformation vector. For a linear elastic material, the constitutive equation defined as

$$\boldsymbol{\sigma} = \mathbf{C} : \boldsymbol{\varepsilon} \tag{12}$$

where $\mathbf{C}$ is the isotropic elastic moduli matrix. To retrieve the term $\mathbf{K_i^{-1}}(\mathbf{x_j} - \mathbf{x_i})$ in Eq. (6), $\mathbf{Q}^*$ is defined as

$$\mathbf{Q}^* = \begin{bmatrix} Q_1 & 0 & Q_2 \\ 0 & Q_2 & Q_1 \end{bmatrix} \quad \text{(2D)} \tag{13}$$

$$\mathbf{Q}^* = \begin{bmatrix} Q_1 & 0 & 0 & 0 & Q_3 & Q_2 \\ 0 & Q_2 & 0 & Q_3 & 0 & Q_1 \\ 0 & 0 & Q_3 & Q_2 & Q_1 & 0 \end{bmatrix} \quad \text{(3D)} \tag{14}$$

where $\mathbf{Q_{ij}} = \mathbf{K_i^{-1}}\left(\mathbf{x_j} - \mathbf{x_i}\right) = [Q_1, Q_2]$ for 2D and $[Q_1, Q_2, Q_3]$ for 3D. Finally, the force vectorstate is obtained by

$$\mathbf{T_i}\langle \mathbf{x_j} - \mathbf{x_i} \rangle = \omega_{ij} \mathbf{Q_{ij}^*} \boldsymbol{\sigma}_i \tag{15}$$

Zero-Energy Mode

NOSB-PD suffers from an instability problem, known as a "zero-energy mode" mechanism [39,42]. It is mainly observed in regions with high strain gradients. The term "zero-energy mode" associated with

reference to the Finite Element Analysis (FEA) refers to a nodal displacement vector that is not a rigid-body motion, yet produces zero strain energy. Instabilities arise because of weak-form element formulation processes such as the use of a low-order Gauss quadrature rule. Certain higher-order polynomial terms vanish at Gauss points, thus eliminating these terms from contribution to the system stiffness [43, 44].

In the context of peridynamics, the zero-energy mode is associated to a weak coupling of material points with their surrounding points and thus results in oscillations in the deformation and stress fields. The zero-energy mode is also present in the other available meshfree methods such as smoothed particle hydrodynamics (SPH) and element-free Galerkin method (EFG).

The definition of the zero-energy mode has been given by Breitenfeld et al. [39] and described herein. Consider a rigid-body with a deformation vector-state, $\mathbf{Y}$, and its approximate deformation gradient tensor of $\mathbf{F}$. For an interior point $\mathbf{x}$, away from the boundaries, a symmetric horizon provides $\int_{H_\mathbf{x}} \omega(|\boldsymbol{\xi}|)\boldsymbol{\xi} dV_{\mathbf{x}'} = 0$. While holding all other points fixed, an arbitrary displacement, $\hat{\mathbf{u}}$, in the point $\mathbf{x}$, yields a new deformation state of $\hat{\mathbf{Y}}(\boldsymbol{\xi}) = \mathbf{Y}(\boldsymbol{\xi}) - \hat{\mathbf{u}}$. The corresponding approximate deformation gradient tensor, $\hat{\mathbf{F}}$, is obtained by

$$\hat{\mathbf{F}} = \mathbf{F} - \hat{\mathbf{u}} \otimes \left(\int_{H_\mathbf{x}} \omega(|\boldsymbol{\xi}|)\boldsymbol{\xi} dV_{\mathbf{x}'} \right) . \mathbf{K}^{-1} = \mathbf{F} \tag{16}$$

This indicates that the arbitrary displacement, $\hat{\mathbf{u}}$, results in no strain energy as calculated by the approximate deformation gradient tensor presented in Eq. (16). The presence of the zero-energy modes results in fictitious solutions (e.g., oscillations in the stress and strain fields) that are not physically explained. Therefore, the zero-energy mode may affect the failure and damage pattern. There are a few methods to alleviate this problem. Decreasing the particle spacing is one of available treatments which may reduce the zero-energy mode oscillations. For dynamic problems, providing artificial viscosity in the NOSB-PD equation of motion is also mentioned to alleviate the zero-energy mode oscillations [45]. However, another level of effort is required to significantly reduce the undesired oscillations. Several other methods have been developed by Littlewood [46], Breitenfeld et al. [39], and Wu and Ren [47] to suppress the zero-energy mode.

The methods developed by Littlewood [46] and Breitenfeld et al. [39] share the fundamental notion that a supplementary force introduced into the force vector-state in peridynamics ($\mathbf{T}_{ZE}$ in Eq. 17) can relieve the zero-energy mode, although the definition of the supplementary forces vary in their models. Littlewood [46] defined a penalty term based on differences between the actual position of each particle and its numerical position predicted by the nonlocal deformation gradient tensor. Therefore, the supplementary force is defined proportional to the penalty term. Breitenfeld et al. [39] introduced two approaches for the supplementary term. In the first approach, the extra force is proportional to the relative displacement of the bond, whereas in the second approach, it is proportional to the averaged displacement of all other particles in the horizon.

$$\mathbf{T}_{\boldsymbol{i}}\langle \mathbf{x}_{\boldsymbol{j}} - \mathbf{x}_{\boldsymbol{i}} \rangle = \omega_{ij} \boldsymbol{\sigma}_i \mathbf{K}_{\boldsymbol{i}}^{-\mathbf{1}} \left(\mathbf{x}_{\boldsymbol{j}} - \mathbf{x}_{\boldsymbol{i}} \right) + \mathbf{T}_{ZE}\langle \mathbf{x}_{\boldsymbol{j}} - \mathbf{x}_{\boldsymbol{i}} \rangle \tag{17}$$

Breitenfeld et al. [39] listed three possible forms for the $\mathbf{T}_{ZE}\langle \mathbf{x}_{\boldsymbol{j}} - \mathbf{x}_{\boldsymbol{i}} \rangle$ as below, where C_I , C_{II} and C_{III} are constants and required to be obtained. K is the bulk modulus and $\mathbf{h} = (\mathbf{F} - \mathbf{I})\left(\mathbf{x}_j - \mathbf{x}_i\right) - (\mathbf{u}_j - \mathbf{u}_i)$ is the hourglass vector.

$$\mathbf{T}_{ZE}\langle \mathbf{x}_j - \mathbf{x}_i \rangle = C_I \omega_{ij} (\mathbf{u}_j - \mathbf{u}_i) \tag{18}$$

$$\mathbf{T}_{ZE}\langle \mathbf{x}_j - \mathbf{x}_i \rangle = C_{II} \sum_{j=1}^{n_i} \omega_{ik} (\mathbf{u}_k - \mathbf{u}_i) V_k \tag{19}$$

$$\mathbf{T}_{ZE}\langle \mathbf{x}_j - \mathbf{x}_i \rangle = -C_{III} \left(\frac{18K}{\pi \delta^4} \right) \mathbf{h}. (\mathbf{y}_j - \mathbf{y}_i) \frac{\mathbf{y}_j - \mathbf{y}_i}{|\mathbf{y}_j - \mathbf{y}_i|^2} V_i V_j \tag{20}$$

These expressions introduce a spring-like bond forces to give an additional coupling of a material point with its neighboring points. In the first method (Eq. 18), the spring-like bond force is calculated simply as

a function of relative displacement of the bond. In the second method (Eq. 19), the average of relative displacement over all bonds around the point is used in calculation of the force. In the third form (Eq. 20) originally developed by Littlewood [46], the additional force vector-state term is based on the penalty term. It is noteworthy that the performance of each method is highly dependent on the spring coefficients, C_I , C_{II} and C_{III}. Evidently, it becomes ineffective to use a very small spring coefficient in controlling zero-energy mode. On the other hand, for too large spring coefficients, the spring force dominates the solution [39], and it can lead to a numerical divergence. Therefore, an optimum value of the spring coefficient needs to be adjusted based on material model and the discretization scheme such as point spacing and horizon size, and the shape of a weight function. As a result, multiple attempts are required to determine a suitable spring coefficient for each problem.

Wu and Ren [47] introduced a control method for suppressing zero-energy mode by replacing the deformation field, $\mathbf{u}_i$, by the stabilized displacement field, $\overline{\mathbf{u}}_i$, defined by Eq. (21), where $\bar{\omega}_{ij}$ is the modified weight function and takes the form of normalized weight function as shown in Eq. (22).

$$\overline{\mathbf{u}}_i = \sum_{j=1}^{n_i} \bar{\omega}_{ij} \mathbf{u}_j V_j \tag{21}$$

$$\bar{\omega}_{ij} = \frac{\omega_{ij}}{\sum_{j=1}^{n_i} \omega_{ik} V_k} \tag{22}$$

The stabilized displacement of each particle is determined by providing weighted average displacement of all other particles and yields reduced oscillations in the deformation field. The approach eliminated the need to obtain the spring coefficient. However unfortunately, the oscillation problem remains in the strain and stress fields with the Wu and Ren model.

Yaghoobi and Chorpeza [17] proposed a method where higher order terms are contained in the formulation by using certain influence functions. Tupek and Radovitzky [18] proposed using different strain measures in the model.

Other types of solutions to the instability issues have been proposed such as the stress-point method [19] and the scheme by Chowdhury et al. [20]. A stabilization type that has been explored in recent times is stabilization by bond association, where kinematic quantities are associated to PD bonds instead of the PD material points. The bond-level stabilization [21], and the bond-associated stabilization [22,23] show the effectiveness of this type of stabilization technique.

In particular, the bond-associated stabilization, by Chen et al. [22,23] has shown very good performance in stabilizing the solutions in an inherent way, without tuning parameters. Moreover, the implementation is quite straightforward. The deformation gradient and force state are computed for each bond, and are therefore called bond-associated deformation gradient and bond-associated force state. The method has been applied in the context of the weak form of peridynamics for linear elastic models [24], in hyperelastic material models with rupture [25–27], in concrete spalling computations [28], as well as in multiphysics problems, such as the linear piezoelectricity PD implementation [29]. Also, the wave dispersion property of the model has also been subject of study in [30].

References

[1] S. A. Silling, Reformulation of elasticity theory for discontinuities and long-range forces, Journal of the Mechanics and Physics of Solids 48 (1) (2000) 175-209.

[2] S. A. Silling, E. Askari, A meshfree method based on the peridynamic model of solid mechanics, Computers & Structures 83 (17) (2005) 1526-1535.

[3] F. Bobaru, M. Yang, L. F. Alves, S. A. Silling, E. Askari, J. Xu, Convergence, adaptive refinement, and scaling in 1d peridynamics, International Journal for Numerical Methods in Engineering 77 (6) (2009) 852-877.

[4] Y. D. Ha, F. Bobaru, Studies of dynamic crack propagation and crack branching with peridynamics, International Journal of Fracture 162 (1-2) (2010) 229-244.

[5] F. Bobaru, Y. D. Ha, Adaptive refinement and multiscale modeling in 2d peridynamics.

[6] W. Hu, Y. D. Ha, F. Bobaru, S. A. Silling, The formulation and computation of the nonlocal j-integral in bond-based peridynamics, International journal of fracture 176 (2) (2012) 195-206.

[7] W. Liu, J.-W. Hong, Discretized peridynamics for brittle and ductile solids, International Journal for Numerical Methods in Engineering 89 (8) (2012) 1028-1046.

[8] F. Bobaru, W. Hu, The meaning, selection, and use of the peridynamic horizon and its relation to crack branching in brittle materials, International Journal of Fracture (2012) 1-8.

[9] M. Tupek, J. Rimoli, R. Radovitzky, An approach for incorporating classical continuum damage models in state-based peridynamics, Computer Methods in Applied Mechanics and Engineering 263 (2013) 20-26.

[10] E. Askari, F. Bobaru, R. Lehoucq, M. Parks, S. Silling, O. Weckner, Peridynamics for multiscale materials modeling, in: Journal of Physics: Conference Series, Vol. 125, IOP Publishing, 2008, p. 012078.

[11] H. Ren, X. Zhuang, Y. Cai, T. Rabczuk, Dual-horizon peridynamics, International Journal for Numerical Methods in Engineering.

[12] K. Yu, Enhanced integration methods for the peridynamic theory, Ph.D. thesis, Citeseer (2011).

[13] W. Gerstle, N. Sau, S. Silling, Peridynamic modeling of concrete structures, Nuclear engineering and design 237 (12) (2007) 1250-1258.

[14] S. A. Silling, M. Epton, O. Weckner, J. Xu, E. Askari, Peridynamic states and constitutive modeling, Journal of Elasticity 88 (2) (2007) 151-184.

[15] T. L. Warren, S. A. Silling, A. Askari, O. Weckner, M. A. Epton, J. Xu, A non-ordinary state-based peridynamic method to model solid material deformation and fracture, International Journal of Solids and Structures 46 (5) (2009) 1186-1195.